PHYSICAL REVIEW B VOLUME 14, NUMBER 4 15 AUGUST 1976

Electron-hole droplets and impurity band states in heavily doped Si(P): Photoluminescence experiments and theory

B. Bergersen, J. A. Rostworowski, M. Eswaran, and R. R. Parsons
Department of Physics, The University of British Columbia, Vancouver, British Columbia, Canada, V6T 1W5

P. Jena
Department of Physics, Northwestern University, Evanston, Illinois 60201
(Received 18 March 1976)

The photoluminescence spectrum of phosphorus-doped silicon at dopant concentrations ranging from 1.2×10^{17} cm^{-3} to 4×10^{19} cm^{-3} is studied as a function of excitation power. The results are interpreted in terms of recombination of charge carriers inside an electron-hole drop and of a free hole with an electron loosely bound to an impurity site. Comparison is made with theoretical estimates of the impurity band density of states outside the drop and improved estimates of the charge carrier density and threshold energy associated with the electron-hole liquid.

I. INTRODUCTION

In the semiconductors Si and Ge a high density of nonequilibrium carriers is known to condense to form macroscopic droplets of liquid known as the "electron-hole droplet" (EHD).[1] The ground-state properties of the EHD in the case of intrinsic material have been extensively studied both experimentally[2,3] and theoretically[4-7] and the agreement between theory and experiment is very good. Recent photoluminescent studies by Halliwell and Parsons[8] indicate that the EHD is observed in phosphorus-doped silicon at quite high dopant concentrations, even above the critical concentration $n_{crit}\simeq3\times10^{18}$ cm^{-3} for the semiconductor-metal transition. However, these results were not obtained with good signal-to-noise ratio and therefore the interpretation of the data did not permit a detailed analysis of the line shapes, especially for dopant concentrations near and above n_{crit}. As the experimental section outlines below, we have rebuilt our apparatus and are now able to obtain well-resolved spectra with good signal-to-noise ratio at all impurity concentrations of interest and over a wide range of excitation power. A preliminary account of the experimental results has been already reported.[9] Here we present a complete description of the experiment and data together with a theoretical treatment.

A theory for the ground-state properties of the EHD in heavily doped Ge and Si has been presented by Bergersen *et al.*[10] Good agreement was found between the theoretical and experimental values of the threshold energy associated with radiation from recombination inside the liquid. The theory of Ref. 10 was developed for the high impurity concentration domain above the semiconductor-metal transition although the agreement with experiment on Si(P) actually turns out to be fair for all densities.

When it comes to the line shape there exists in addition to Ref. 10 a more phenomenological theory by Mahler and Birman.[11] As mentioned above, the low signal-to-noise ratio for the experimental results did not permit a detailed line-shape analysis. However, the half-widths of the observed peaks were found to be in qualitative agreement with theory.

By studying the photoluminescent spectrum of Si(P) as a function of the excitation level we are able to analyze the spectrum as a sum of two spectra. The first of these is interpreted in terms of recombination inside the EHD; the second, in terms of recombination of free holes with electrons in the "impurity band."[12] At low excitation intensity the droplets are few and far apart and most recombination events are of the latter type. As the excitation intensity is increased the droplet line grows. An important aspect of the present paper is to show that by studying the spectra at various excitation intensities the two types of lines can be disentangled and a comparison made between experiment and theory for the different types of recombination.

Section II contains a summary of our theoretical treatment of the EHD in heavily doped material. New numerical results are presented for the threshold energy and charge-carrier concentrations taking into account some of the effects neglected in Ref. 10. When these methods are extended to lower impurity concentrations an interesting feature of the results is a dip in the charge-carrier densities inside the drop for intermediate dopant concentrations. Some insight into why this dip occurs can be found by looking at the energetics of the situation in the Hartree-Fock ap-

proximation and a discussion of this point is given in the Appendix. We expect that if the impurity contribution to the energy had been calculated more accurately the effect would have become much less pronounced. The experimentally observed dip in the minority carrier concentration is also quite shallow.

In Sec. III we discuss the density of states in the impurity band. For very low impurity concentrations the impurity states can be described in terms of the discrete energy levels of the isolated impurities. With increasing impurity concentration the wave functions of the donor electrons centered at different sites start to overlap and one gets an impurity band.

At moderately low impurity concentration one can treat the lowest-lying impurity states in the tight-binding approximation. The Coulomb repulsion between electrons makes it energetically unfavorable for two impurity electrons to occupy the same site and this interaction will be treated in the Hubbard[13] model. We are not aware of any calculations in the literature which adequately take into account both the Coulomb repulsion between electrons and the randomness of the impurity distribution. For this reason we follow the treatment of Berggren[14] and assume that the donors form a regular lattice and use the Hubbard model for the electron interactions.

As one increases the dopant concentration beyond the critical density n_{crit}, correlation effects associated with the electron-electron repulsion become relatively less important while there continue to be significant effects due to the randomness of the impurity distribution on the charge-carrier densities of state. We expect that the main effect of this is to produce "tails" in the energy bands. No numerical estimates of the band tailing will be presented here.

The experimental setup is described in Sec. IV. The experimental results and the analysis of the data are presented in Sec. V. A summary is presented in Sec. VI.

II. THEORY OF THE ELECTRON-HOLE LIQUID IN HEAVILY DOPED MATERIAL

A. Model

We represent the Si conduction band by a six-valley structure centered at

$$\vec{k}_0 = (2\pi/a)(0.85, 0, 0)\ , \tag{1}$$

and equivalent points. Here $a = 5.43$ Å. Near the bottom of these valleys the conduction band will be treated in the effective-mass approximation.[15,16] We have taken the values $m_{lc} = 0.91 m_0$ and $m_{tc} = 0.19 m_0$ for the longitudinal and transverse effective masses. The conduction-electron wave functions can be written in the Bloch form

$$\psi_{n\vec{k}}(\vec{r}) = \Omega^{-1/2} u_{n\vec{k}}(\vec{r})\, e^{i\vec{k}\cdot\vec{r}}\ , \tag{2}$$

with Ω denoting the volume of the crystal. It is useful to expand the periodic function

$$u^*_{n\vec{k}}(\vec{r})\, u_{n\vec{k}'}(\vec{r}) = \sum_{\vec{K}_m} C^{nn}_{\vec{k}\vec{k}'}(\vec{K}_m)\, e^{-i\vec{K}_m\cdot\vec{r}}\ , \tag{3}$$

where $\vec{K}_m$ are the reciprocal-lattice vectors. In this notation,[16] matrix elements of one-body operators of the form

$$U(\vec{r}) = \sum_{\vec{q}} U(\vec{q})\, e^{i\vec{q}\cdot\vec{r}} \tag{4}$$

can be written

$$\langle n\vec{k}\,|\,U\,|\,n\vec{k}'\rangle = \sum_{\vec{K}_m} U(\vec{k}-\vec{k}'+\vec{K}_m)\, C^{nn}_{\vec{k}\vec{k}'}(\vec{K}_m)\ . \tag{5}$$

As long as we restrict the wave vectors to lie in the same valley we can put

$$C^{nn}_{\vec{k}\vec{k}'}(0) \approx 1\ , \tag{6}$$

and the terms $C^{nn}_{\vec{k}\vec{k}'}(K_m)$ with $m \neq 0$ are small in comparison. It is then a good approximation to put

$$\langle n\vec{k}\,|\,U\,|\,n\vec{k}'\rangle \approx U(\vec{k}-\vec{k}')\ . \tag{7}$$

However, when it comes to evaluating the matrix elements of the Coulomb interaction between states in different valleys (7) does not appear to be a good approximation. There will always be one nonzero reciprocal-lattice vector $\vec{K}_m$ such that $|\vec{k}-\vec{k}'-\vec{K}_m| < |\vec{k}-\vec{k}'|$, i.e., the most dominant contribution to the sum in (5) does not necessarily come from the $\vec{K}_m = 0$ term. Nevertheless, approximation (7) is known empirically to give good results for the impurity energies[16] in Si(P). We hope elsewhere to be able to present results based on (5) without the approximation (7). In the present paper we are only interested in intervalley terms in order to check whether they are negligible or not and for this purpose (7) is adequate.

The valence bands will be described in terms of light and heavy holes with masses $m_{\text{lh}} = 0.16 m_0$ and $m_{\text{hh}} = 0.48 m_0$, respectively. Coulomb matrix elements between states in the valence bands are treated as described by Combescot and Nozières.[4,17] This means that we neglect any nonparabolicity of the valence bands, but take into account the coupling between the two top valence bands. Since we will only be concerned with n-type impurities, the hole concentration will never become so large that it will become necessary to take into account the $j = \frac{1}{2}$ valence band.

The Coulomb interaction between the charge carriers is screened by the dielectric function of the host. We make use of the simplified analytic form suggested by Nara and Morita[18]

$$\frac{1}{\epsilon(q)} = A\,\frac{q^2}{q^2+\alpha^2} + \frac{(1-A)\,q^2}{q^2+\beta^2} + \frac{\epsilon^{-1}(0)\,\gamma^2}{q^2+\gamma^2}\ , \tag{8}$$

with $A = 1.175$, $\alpha = 0.7572$ a.u., $\beta = 0.3123$ a.u., $\gamma = 2.044$ a.u., and $\epsilon(0) = 11.4$.

We next turn to the energetics of electron-hole drop formation. Let n_d represent the concentration of impurity electrons and n_h the number of valence band holes per unit volume inside the electron-hole liquid. We only consider here the case where the drops formed are large enough for the surface energy to be small compared with the bulk energy so that we can assume the drops to be approximately charge neutral. This allows us to put $n_c = n_h + n_d$ for the total density of electrons. Next, let $E(n_c, n_h)$ be the total energy per unit volume, i.e., the sum of the kinetic, exchange, correlation, and impurity energies associated with the indicated densities:

$$E(n_c, n_h) = E_{\rm kin}(n_c, n_h) + E_{\rm exc}(n_c, n_h) + E_{\rm corr}(n_c, n_h) + E_{\rm imp}(n_c, n_h)\ . \tag{9}$$

Suppose the volume of the crystal is Ω and there is an electron-hole drop of volume V inside the crystal. The total energy is then

$$E(\text{crystal}) = (\Omega - V)\,E(n_d, 0) + VE(n_d + n_h, n_h)\ . \tag{10}$$

At low temperatures the hole density n_h will be determined by the requirement that (10) be a minimum, subject to the constraint that the total number $N = Vn_h$ of excess charge-carrier pairs be kept constant. This leads to the exact condition for equilibrium

$$\bar{E}(n_d, n_h) \equiv (1/n_h)\,[E(n_d + n_h, n_h) - E(n_d, 0)] = \text{minimum}\ . \tag{11}$$

Stated otherwise Eq. (11) implies that the average energy per excess charge-carrier pair inside the drop should be a minimum. At this quasiequilibrium we have

$$\bar{E}(n_d, n_h) = E_{\rm pair} \equiv \frac{\partial}{\partial n_h}\,E(n_d + n_h, n_h)\ , \tag{12}$$

i.e., the average energy $\bar{E}$ per pair inside the liquid has to be the same as the energy $E_{\rm pair}$ required to add one extra electron-hole pair. The latter quantity can be determined from the high-energy threshold of the droplet luminescence line. Throughout this calculation our unit of energy is the "exciton Rydberg"

$$R_0 = m_A e^4/2\hbar^2\epsilon^2 = 13.1\ \text{meV}, \tag{13}$$

where

$$m_A = \left[\tfrac{1}{3}(m_{lc}^{-1} + 2\,m_{tc}^{-1}) + \tfrac{1}{2}(m_{\rm hh}^{-1} + m_{\rm lh}^{-1})\right]^{-1} = 0.124\,m_0\ . \tag{14}$$

The impurity, hole, and conduction-electron densities are parametrized by the quantities r_d, r_h, and r_c given by

$$\frac{4\pi a_0^3}{3}\times\begin{Bmatrix} r_d^3 \\ r_c^3 \\ r_h^3 \end{Bmatrix} = \begin{Bmatrix} n_d^{-1} \\ n_c^{-1} \\ n_h^{-1} \end{Bmatrix}\ , \tag{15}$$

where

$$a_0 = \epsilon\hbar^2/m_A e^2 = 48.6\ \text{Å} \tag{16}$$

is the exciton Bohr diameter.

B. Calculation of $E(n_c, n_h)$

1. Kinetic and exchange energies

The kinetic and exchange contributions to the energy density will in the present calculation be computed as described in Refs. 4 and 10. We give the formulas in the Appendix. The calculation neglects the energy due to intervalley exchange. A proper calculation of this contribution would involve summing up terms involving different reciprocal-lattice vectors as discussed in connection with (5). Such a calculation would be rather complicated and in order to estimate the possible significance of intervalley exchange let us instead make the effective-mass approximation (7). This gives for the conduction-electron exchange energy per unit volume, with $f^-(\vec{k})$ as the Fermi distribution function,

$$E_{\rm exc}^c(n_c) = \frac{1}{(2\pi)^6}\int d^3k \int d^3k'\,\frac{4\pi e^2 f^-(\vec{k})\,f^-(\vec{k}')}{\epsilon(\vec{k}-\vec{k}')\,|\vec{k}-\vec{k}'|^2}\ . \tag{17}$$

Equation (17) can be separated into an inter- and intravalley part. In the latter case the momentum transfer $|\vec{k}-\vec{k}'|$ will never be very large and we have neglected the wave-vector dependence of the dielectric function in the intravalley term. In the intervalley contribution $\vec{k}$ and $\vec{k}'$ lie in different valleys and the wave-vector dependence of $\epsilon(\vec{k})$ is quite important. If k_i is the distance from the Γ point to any of the valley minima we then must either have $|\vec{k}-\vec{k}'| \approx k_1 = \sqrt{2}\,k_i$, or $|\vec{k}-\vec{k}'| \approx k_2 = 2k_i$. With this approximation the intervalley contribution to (17) can easily be evaluated to yield

$$\frac{\pi}{24}\,\frac{e^2 n_c^2}{k_i^2}\left(\frac{8}{\epsilon(k_1)} + \frac{1}{\epsilon(k_2)}\right). \tag{18}$$

What matters in the present calculation is not the absolute value of the different contributions to the energy, but their effect on the derivative of the energy with respect to the minority carrier density [see Eq. (12)]:

$$E_{\text{pair}}(\text{intervalley exch}) = \frac{\pi}{12}\frac{e^2 n_c}{k_i^2}\left(\frac{8}{\epsilon(k_1)} + \frac{1}{\epsilon(k_2)}\right). \tag{19}$$

At $n_d = 4\times10^{19}$ cm^{-3} Eq. (19) represents 2% of E_{pair} and its importance is even less for lower impurity densities [e.g., Eq. (19) represents 0.15% of E_{pair} at the critical density n_{crit}]. We therefore felt justified in neglecting the intervalley contribution to the exchange energy in our determination of n_h and E_{pair} at quasiequilibrium.

2. *Correlation energy*

We will (as was done in Ref. 10), calculate the correlation energy inside the electron-hole drop in the random-phase approximation (RPA). Our treatment differs from that of previous work in that we have replaced the dielectric constant ϵ of the pure host by a wave-vector dependent dielectric function. This gives

$$E_{\text{corr}}(n_c, n_h) = \frac{1}{2}\int\frac{d^3q}{(2\pi)^3}\int_{-i\infty}^{i\infty}\frac{d\omega}{2\pi i}\left[\frac{4\pi e^2}{\epsilon(q)q^2}S(\vec{q},\omega) + \ln\left(1 - \frac{4\pi e^2}{\epsilon(q)q^2}S(\vec{q},\omega)\right)\right]. \tag{20}$$

Here $S(\vec{q},\omega)$ is the pair correlation function which in the present work is evaluated as described in detail in Ref. 10. The replacement of the dielectric constant by a dielectric function will give greater emphasis to the large q contributions. The resulting change in E_{pair} is quite small (a few percent). Since the RPA is not a good approximation at large momentum transfer, we have made no attempt to include intervalley corrections to (20) in our calculations.

In the case of intrinsic material Bhattacharyya *et al.*[7] argue that one can expect corrections to E_{corr} that go beyond the random-phase approximation to amount to slightly above 20% of E_{pair}. These corrections will become less important when the charge-carrier concentration is higher than the concentration within the EHD of pure Si, and the percentage error must be expected to be larger than this for lower carrier concentrations. The corrections to E_{corr} will have the effect of making this quantity more negative. Let us now consider the two terms $E(n_d+n_h, n_h)$ and $E(n_d, 0)$ which enter in E_{pair}. For very low impurity concentrations the percentage error in $E(n_d, 0)$ will be large, but since this term will be very small compared to $E(n_d+n_h, n_h)$ this will be of little consequence. The effect of corrections to the RPA correlation energy must then be about the same as in the intrinsic case. However, when considering impurity densities which are of the same order of magnitude as the quasiequilibrium n_h the absolute error in $E(n_d, 0)$ could well become just as large or even larger than the error in $E(n_d+n_h, n_h)$. For this reason the errors must be expected to cancel out to a considerable degree—or one could even have a situation where a calculated correlation energy which is not negative enough leads to a calculated E_{pair} which is too negative. Similar cancellation effects are expected to play a role in the impurity energy contribution to be discussed later and they probably contribute significantly to the quite good agreement obtained between the theoretical value for E_{pair} and the location of the high-energy edge of the droplet luminescence line that we have obtained experimentally. Finally, if we go to very high impurity concentrations the RPA will become a very good approximation and the correction term correspondingly small.

3. *Impurity energy*

We will, as was done in Ref. 10, assume that the phosphorus impurities are linearly screened randomly distributed point charges. Since the "jellium" contribution to the impurity energy already is included in the correlation term the major part of E_{imp} will be an intravalley term which is of second order in the charge-carrier–impurity interaction and which involves a carrier interacting twice with the same site,

$$E_{\text{imp}}(n_c, n_h) = \frac{2\pi Z e^2 n_d}{(2\pi)^3} \times\int\frac{d^3q}{\epsilon(\vec{q})q^2}\,\frac{4\pi e^2\,\epsilon^{-1}(\vec{q})\,S(\vec{q},0)}{[q^2 - 4\pi e^2\,\epsilon^{-1}(\vec{q})\,S(\vec{q},0)]}. \tag{21}$$

This equation differs from the corresponding result in Ref. 10 in that we have attempted to include "central-cell corrections" by replacing the host dielectric constant by a wave-vector dependent $\epsilon(\vec{q})$. Equation (21) is linear in the impurity concentration. There is another second-order contribution involving a carrier interacting with two different impurity sites. This term is quadratic

in the impurity concentration and can only be expected to be important at very high impurity concentrations. In order to estimate it we write the impurity-impurity interaction in the form

$$E^{dd} = \tfrac{1}{2} P_d n_d \frac{1}{\Omega} \sum_{\vec{q}, l \neq 0} v_{\vec{q}} e^{i \vec{q} \cdot \vec{R}_l} . \tag{22}$$

Here the sum over l is a sum over all sites in the crystal and $P_d = n_d/\mathcal{N}$ is the probability that this site is occupied by a phosphorus ion. $\mathcal{N}$ is the number of sites per unit volume of the crystal and $v_{\vec{q}}$ is the Fourier transform of a screened impurity-impurity interaction. Equation (22) can be rewritten

$$E^{dd} = \tfrac{1}{2} n_d^2 \sum_{\vec{K}_n \neq 0} \left(v_{\vec{K}_n} - \frac{1}{\mathcal{N}\Omega} \sum_{\vec{q}}^{BZ} v_{\vec{q}+\vec{K}_n} \right) - \frac{1}{2} \frac{n_d^2}{\mathcal{N}\Omega} \sum_{\vec{q}}^{BZ} v_{\vec{q}} . \tag{23}$$

The superscript BZ indicates that the sum is restricted to the first Brillouin zone.

We are only interested in the contribution of (23) to E_{pair}, i.e., to the derivative of the energy with respect to the minority charge-carrier density inside and outside the droplet. This contribution comes about because the screening of the impurities is more efficient if there are more free charge carriers present. Only the contribution from the first Brillouin zone is important for this screening. We can thus approximate

$$E^{dd}_{\text{pair}} \approx \frac{n_d^2}{\mathcal{N} 4\pi^2} \int_0^\infty q^2 \, dq \, \frac{\partial}{\partial n_h} v_q (n_d + n_h, n_h) . \tag{24}$$

If we next put

$$v_q = \frac{4\pi e^2/\epsilon(q)}{q^2 + [4\pi e^2/\epsilon(q)] S(q, 0)} \approx \frac{4\pi e^2/\epsilon(0)}{q^2 + [4\pi e^2/\epsilon(0)] S(0, 0)} , \tag{25}$$

we can easily evaluate (24) to give

$$E^{dd}_{\text{pair}} \approx \frac{e^2 n_d^2}{8\epsilon(0)} \left(\frac{1}{\mathcal{N}} \right) \frac{1}{\sqrt{s}} \frac{\partial s}{\partial n_h} , \tag{26}$$

where $s = -4\pi e^2 S(0, 0)/\epsilon(0)$. At the highest impurity concentration considered here (4×10^{19} cm^{-3}), Eq. (26) is 1% of E_{pair} and the contribution falls off fairly rapidly with decreasing impurity concentration. Since this term is very small we have neglected it in our energy minimization calculation.

There are other corrections to (21) which are more serious. Even at dopant concentrations as high as several times n_{crit} it is believed that the charge-carrier states have some localized character.[19] At still lower densities the tight-binding approach of Sec. III is more appropriate. In order to illustrate this point we show in Fig. 1 how the average energy per impurity electron varies with the impurity concentration. At low impurity concentrations this quantity should approach the ionization energy of the lowest impurity state in Si(P). Experimentally[20] the energy of the impurity state is found to be -45.3 meV. When the methods of Pantelides and Sah[16] are used to calculate this energy we get -46.9 meV (see also Sec. III). This value was obtained taking into account intervalley terms in the approximation (7). If intervalley terms had been neglected one would have obtained the value -31 meV for the impurity ground-state energy. Equation (21) was evaluated without taking into account intervalley terms. It is easy to make a crude estimate of the neglected effect in the same spirit as was done in going from (17) to (19). However, the effect will now be very small because the terms will contain factors proportional to k_1^{-4} or k_2^{-4}.

We conclude that Eq. (21) will lead to a fairly gross underestimate of the impurity energy except at the very highest densities considered. However, there will be the same type of cancellation effect that we discussed in connection with the correlation energy. The error in the calculated value of

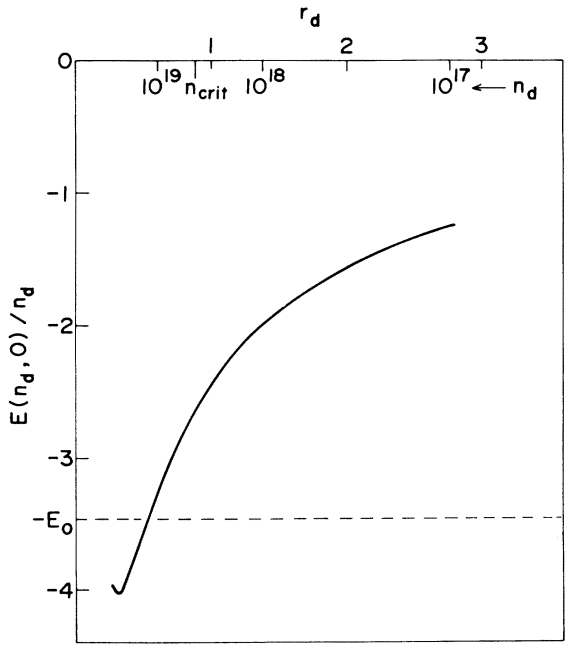

FIG. 1. $E(n_d, 0)/n_d$, the energy per donor outside the droplet as obtained by adding the kinetic, exchange, and correlation energies, is shown as a function of the impurity concentration n_d. $-E_0$ denotes the binding energy of the isolated donor in it ground state. The energy is in units of R_0, the excitonic rydberg.

E_{pair} will therefore be much smaller than could be expected from a quick glance at Fig. 1.

C. Calculation of n_h and E_{pair}

The different contributions to $\bar{E}(n_d, n_h)$ in Eq. (12) were evaluated numerically from (A1), (20), and (21) for different impurity and excess charge-carrier densities. For each value of n_d we found the value of n_h for which $\bar{E}$ had a minimum. The resulting values of E_{pair} and n_h are plotted in Figs. 2 and 3, respectively, and compared to previous results.[21] In Fig. 3 we also plot the majority carrier density inside the drop for different impurity concentrations. A striking feature of the results is the minimum in n_h and n_c at an intermediate impurity concentration. This minimum was also present in the calculation in Ref. 10 and a similar effect was found by Mahler and Birman.[11,22] We discuss in the Appendix how this minimum comes about by looking at the somewhat simpler Hartree-Fock approximation.

The calculated minimum in the minority charge-carrier density must be treated with a certain scepticism. As discussed in Sec. II B, we expect that in the intermediate density region our calculations significantly underestimate the magnitude

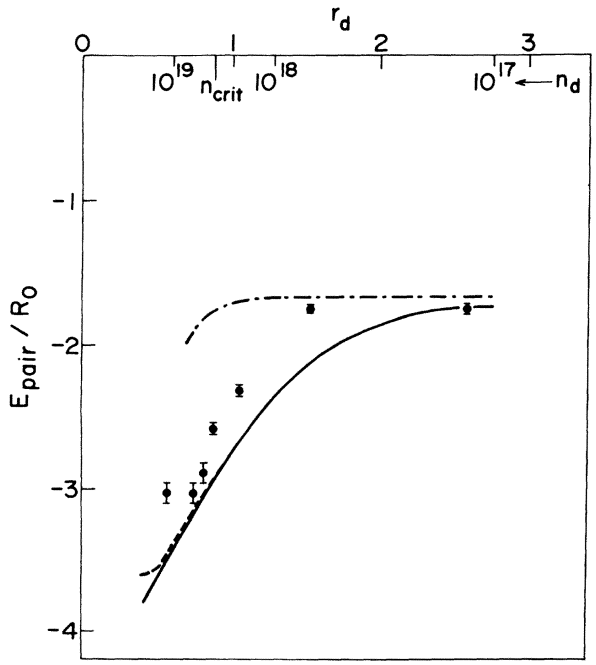

FIG. 2. E_{pair}, the average energy per pair of charge carriers within the droplet, is shown as a function of the impurity concentration n_d. The solid curve denotes the theoretical result obtained in the present work, the dashed line that of Ref. 10. The chained curve is obtained using the ionization energy for $E(n_d, 0)/n_d$. The experimental results are shown as dots with error flags.

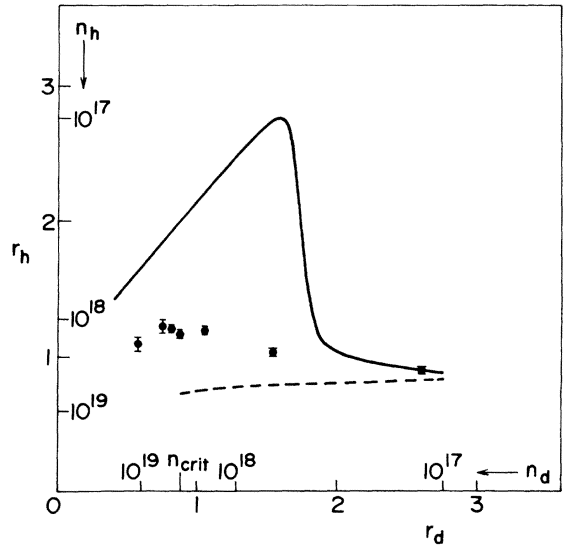

FIG. 3. The equilibrium hole density n_h is shown as a function of the impurity concentration n_d. The solid curve represents the theoretical result with the correlation energy contribution to $E(n_d, 0)$ calculated in the RPA, the dashed curve is the result obtained with $E(n_d, 0)/n_d$ taken to be the experimental ionization energy. The dots with error flags represent the experimental data.

of both the impurity and the correlation energy. We argued that there is likely to be a considerable cancellation of the errors introduced this way. Nevertheless, the minimum in $\bar{E}$ is quite shallow and small errors in the density dependence of $\bar{E}$ could have a significant effect on n_h. This question can be somewhat clarified by the following argument. In the large-U limit of the Hubbard model discussed in Sec. III $(1/n_d)\,E(n_d, 0)$ will be roughly equal to the electronic ground-state energy of the isolated impurity. We have therefore calculated E_{pair} and n_h assuming that

$$E(n_d, 0)/n_d \approx -45.3 \text{ meV}\,, \tag{27}$$

but with $E(n_d + n_h, n_h)$ calculated as before. The results are shown in Figs. 2 and 3. It is seen that the minimum in n_h now has disappeared while the change in E_{pair} is less dramatic. The experimental values of n_h and E_{pair} are discussed in Sec. V.

III. THE IMPURITY BAND

As explained in Sec. II for low impurity concentrations the calculation of the comparison energy $E(n_d, 0)$, i.e., the energy of the donor electrons outside the droplet, is not reliable when obtained in the RPA. Instead, below the density n_{crit} it is reasonable to describe the impurity band in a tight-binding scheme such as the Hubbard model.[13] This model is particularly appropriate because

it is known to exhibit a metal-insulator transition. Apart from $E(n_d, 0)$, we shall also obtain the density of states of the impurity band—a quantity which is directly related to the shape of the photoluminescent peak arising from the recombination of impurity electrons with free holes. The phosphorus impurities will, of course, be randomly distributed but we shall ignore this randomness and following Berggren[14] assume that the impurities are distributed over a simple cubic lattice in the host material. In the Hubbard model the impurity electrons are described by the Hamiltonian

$$H = \sum_{ij\sigma} t_{ij} a^{\dagger}_{i\sigma} a_{j\sigma} + \frac{U}{2} \sum_{i\sigma} n_{i\sigma} n_{i-\sigma}, \tag{28}$$

where $a^{\dagger}_{i\sigma}$ ($a_{i\sigma}$) creates (destroys) an electron with spin σ in a Wannier state at site i, $n_{i\sigma}$ denotes the number operator for electrons of spin σ at site i, t_{ij} is the transfer matrix element between sites i and j, and U is the Coulomb repulsion energy if two donor electrons occupy the same site. Two donor electrons are assumed to interact only when on the same site. We further assume that the transfer matrix element t_{ij} is nonvanishing only when i and j are nearest neighbors.

The transfer matrix element is defined as

$$t_{ij} = \frac{1}{N} \sum_{\vec{k}} E(\vec{k})\, e^{i\vec{k}\cdot(\vec{R}_i - \vec{R}_j)}, \tag{29}$$

where $E(\vec{k})$ is the band energy of the donor electrons when correlations are ignored. We calculate this unperturbed band in the tight-binding scheme. For this we write the Hamiltonian describing the impurity electrons as

$$H = -\frac{\hbar^2}{2m_0} \nabla^2 + V_0(\vec{r}) + \sum_i U(\vec{r} - \vec{R}_i), \tag{30}$$

where $V_0(\vec{r})$ is the periodic potential arising from the host atoms and $U(\vec{r} - \vec{R}_i)$ is the perturbing potential due to an impurity ion at site i:

$$U(\vec{r} - \vec{R}_i) = -e^2/\epsilon |\vec{r} - \vec{R}_i| . \tag{31}$$

Let $\Phi(r)$ denote the ground-state wave function of a donor at an isolated impurity. In principle this is an eigenfunction of the Hamiltonian

$$h = -\hbar^2 \nabla^2 / 2m_0 + V_0(\vec{r}) + U(r) \tag{32}$$

with an energy $-E_0$. Since the impurities are assumed to form a periodic lattice, we describe the impurity band in terms of Bloch functions

$$\Psi_{\vec{k}}(\vec{r}) = \frac{1}{\sqrt{N}} \sum_i a_{\vec{k}}\, e^{i\vec{k}\cdot\vec{R}_i}\, \Phi(\vec{r} - \vec{R}_i) . \tag{33}$$

If we define

$$S_{ij} = \int d^3r\, \Phi^*(\vec{r} - \vec{R}_i)\, \Phi(\vec{r} - \vec{R}_j), \tag{34}$$

and

$$S(\vec{k}) = \frac{1}{N} \sum_i S_{ij}\, e^{-i\vec{k}\cdot\vec{R}_{ij}} , \tag{35}$$

the Bloch functions are normalized provided

$$a_{\vec{k}} = [S(\vec{k})]^{-1/2} . \tag{36}$$

In the tight-binding scheme we have

$$E(\vec{k}) = \langle \Psi_{\vec{k}}(r) | H | \Psi_{\vec{k}}(r) \rangle , \tag{37}$$

which may be written approximately as

$$E(\vec{k}) = \frac{1}{N} \sum_i |a_{\vec{k}}|^2 e^{-i\vec{k}\cdot(\vec{R}_i - \vec{R}_j)} \langle \Phi(\vec{r} - \vec{R}_i) | -\frac{\hbar^2}{2m_0} \nabla^2 + V_0(\vec{r}) + U(\vec{r} - \vec{R}_i) | \Phi(\vec{r} - \vec{R}_j) \rangle$$

$$+ \frac{1}{N} \sum_{\substack{i,j \\ (j \neq i)}} |a_{\vec{k}}|^2 e^{-i\vec{k}\cdot(\vec{R}_i - \vec{R}_j)} \langle \Phi(\vec{r} - \vec{R}_i) | U(\vec{r} - \vec{R}_j) | \Phi(\vec{r} - \vec{R}_j) \rangle, \tag{38}$$

so that

$$E(\vec{k}) = -E_0 + \frac{1}{N} \sum_{\substack{i,j \\ (j \neq i)}} |a_{\vec{k}}|^2 e^{-i\vec{k}\cdot(\vec{R}_i - \vec{R}_j)} \langle \Phi(\vec{r} - \vec{R}_i) | U(\vec{r} - \vec{R}_j) | \Phi(\vec{r} - \vec{R}_j) \rangle . \tag{39}$$

Since the overlap S_{ij} is small in the range of dopant concentrations of interest, we may set $|a_{\vec{k}}|^2 \simeq 1$ in (39). Comparing (29) and (39) we have

$$t_{ij} = \langle \Phi(\vec{r} - \vec{R}_i) | U(\vec{r} - \vec{R}_j) | \Phi(\vec{r} - \vec{R}_j) \rangle, \tag{40}$$

with $j \neq i$. [In the treatment of Berggren,[14] the nonorthogonality term given by (35) and (36) is not treated consistently, and his expression for t_{ij} is different from ours.] Only the hopping matrix element between nearest neighbors is found to be significant. The intra-atomic Coulomb repulsion is given by

$$U = \int d^3r\, d^3r' \mid \Phi(\vec{r})\mid^2 \frac{e^2}{\epsilon\mid \vec{r}-\vec{r}'\mid} \mid \Phi(\vec{r}')\mid^2. \qquad (41)$$

The wave function $\Phi(\vec{r})$ for the ground state of an isolated impurity is obtained in the effective-mass approximation. In this formalism $\Phi(\vec{r})$ is written as a wave packet consisting of Bloch waves, $\phi_{\vec{k}_l}(\vec{r})$, at the six minima $(\vec{k}_l, l = 1, \ldots, 6)$ in the conduction band of silicon:

$$\Phi(\vec{r}) = \sum_{l=1}^{6} \alpha_l F_l(\vec{r}) \phi_{\vec{k}_l}(\vec{r}). \qquad (42)$$

The $F_l(\vec{r})$ are "envelope" functions which are solutions of a well-known effective-mass equation. In the ground state $\alpha_l = 1/\sqrt{6}$ for all l. The envelope functions are hydrogenlike and, because of the anisotropy in the effective mass, may be taken to be of the form

$$F_l(\vec{r}) = \frac{1}{(\pi a^2 b)^{1/2}} \exp\left[-\left(\frac{x^2+y^2}{a^2} + \frac{z^2}{b^2}\right)^{1/2}\right], \qquad (43)$$

with the z axis oriented along the longitudinal axis of the conduction valley at $\vec{k}_l$. Following Miller and Abrahams[23] and Berggren,[14] we take

$$a = \hbar/(2m_t E_0)^{1/2}; \quad b = (m_t/m_l)^{1/2} a, \qquad (44)$$

where E_0 is the observed ionization energy. This choice of a and b gives the correct asymptotic form for $F_l(\vec{r})$, but does not yield (42) as a solution to the effective-mass equation.

With impurity wave functions of the chosen form

$$t_{ij} \simeq \frac{e^2}{6\epsilon a} \sum_{l=1}^{6} e^{-i\vec{k}_l \cdot \vec{R}_{ij}} (1 + R_l/a) e^{-R_l/a}, \qquad (45)$$

where

$$R_l = a\left(\frac{(x_i - x_j)^2}{a^2} + \frac{(y_i - y_j)^2}{a^2} + \frac{(z_i - z_j)^2}{b^2}\right)^{1/2}. \qquad (46)$$

On squaring expression (45) and considering only intravalley terms we get

$$\mid t_{ij}\mid^2 = \left(\frac{e^2}{6\epsilon a}\right)^2 \sum_{l=1}^{6} \left(1 + \frac{R_l}{a}\right)^2 e^{-2R_l/a}. \qquad (47)$$

Upon doing a spherical average over the orientations of $\vec{R}_{ij}$, we obtain

$$\mid t_{ij}\mid^2 \simeq (e^2/6\epsilon a)^2 (A_0 + 2A_1 + A_2), \qquad (48)$$

where

$$A_n = \frac{1}{4\pi} \int d\Omega \left(\frac{R_l}{a}\right)^n e^{-2R_l/a} = \left(\frac{R}{a}\right)^n \int_0^1 dx\, (1+\alpha x^2)^{n/2} e^{-2(R/a)(1+\alpha x^2)^{1/2}}, \qquad (49)$$

with $\alpha = a^2/b^2 - 1$ and $R = \mid \vec{R}_{ij}\mid$. [The expression of Berggren[14] corresponding to (49) contains an algebraic error.]

Finally, using integrals worked out by Miller and Abrahams,[23] Berggren[14] has shown that the intra-atomic Coulomb repulsion is given approximately by

$$U = 5e^2/8\epsilon a. \qquad (50)$$

The value of $\mid t_{ij}\mid$ for the donor concentration 1.8×10^{18} phosphorus cm^{-3} is 1.2 meV. The magnitude of the hopping integral rapidly increases with dopant concentration. The intra-atomic Coulomb repulsion U, which is clearly independent of dopant concentration, is 37.5 meV. As was mentioned earlier, the envelope function (43) gives a reasonable asymptotic behavior but is not accurate in the region close to the donor nucleus, i.e., in the "central-cell" region. Since only the asymptotic behavior of $F(\vec{r})$ is important in the evaluation of the hopping integral (which is a two-center integral) we expect the values thus obtained for $\mid t_{ij}\mid$ to be quite reasonable. In our calculation of U there are two sources of error which have the opposite effect. On the one hand, central-cell corrections [not adequately taken into account in (43)] would increase the magnitude of the wave function close to the nucleus and so tend to increase U. On the other hand, the isolated impurity wave functions would relax considerably on placing two electrons at the same site and this effect would tend to reduce U.

Recently Pantelides and Sah[16] have treated the central-cell corrections to the isolated impurity wave function by using the dielectric function $\epsilon(r)$ in (31) rather than the dielectric constant. They assume a spherically symmetric envelope function of the form

$$F(r) = (\pi a^{*3})^{-1/2} e^{-r/a^*}. \qquad (51)$$

Assuming spherical conduction valleys (with effective mass $m^* = 0.2987 m_0$), on minimizing the expectation value of the isolated impurity Hamiltonian (32), we obtain $a^* = 21.4$ a.u. and an ionization energy 46.9 meV. Pantelides and Sah[16] have used approximations (6) and (7) even for intervalley terms. Consequently, the ground-state wave function obtained is not necessarily reliable in spite of the close agreement of the calculated ionization energy with experiment. Using this wave function we find that $U = 70$ meV and for the donon concentration 1.8×10^{18} phosphorus cm^{-3} $\mid t\mid \simeq 0.26$ meV. The hopping integral is extremely small because the central-cell correction has greatly enhanced the magnitude of the wave function in the neighborhood of the nucleus at the expense of that in the asymptotic region. The value of the intra-atomic Coulomb repulsion

U obtained using the wave function of Pantelides and Sah[16] is unphysically large. With $U = 70$ meV, it would not be possible to bind two donor electrons to the same phosphorus impurity to form a H^--like complex. Dean *et al.*[28] have reported the binding energy of such a complex in Si(P) to be ~4 meV. Since the ionization energy of the neutral donor is 45.3 meV, it follows that $U \sim 41$ meV.

If t and U are known, we can calculate the density of states within the Hubbard model. For the details we refer the reader to Hubbard's original papers.[13] With Hubbard, we approximate the density of states of the original tight-binding band (in the absence of correlations) by the semicircular form

$$\rho_0(E) = \begin{cases} \frac{4}{\pi\Delta}\left[1 - \left(\frac{E - E_0}{\frac{1}{2}\Delta}\right)^2\right]^{1/2}, & \text{if } |E - E_0| < \frac{\Delta}{2} \\ 0, & \text{otherwise,} \end{cases} \tag{52}$$

where $\Delta (= 12|t|)$ is the unperturbed bandwidth.

The pseudoparticle density of states in the Hubbard model when there is one electron per atomic site is then approximately given by the imaginary part of the propagator[13]

$$G(E) = (4/\pi\Delta^2)\{F(E) - [F^2(E) - (\tfrac{1}{2}\Delta)^2]^{1/2}\}, \tag{53}$$

where the quantity $F(E)$ is obtained as the appropriate root of the cubic equation

$$EF^3 - [\tfrac{7}{3}E^2 + \tfrac{3}{4}(\tfrac{1}{2}\Delta)^2 - \tfrac{1}{4}U^2]F^2 + [\tfrac{5}{3}E(E^2 - \tfrac{1}{4}U^2) + \tfrac{3}{2}E(\tfrac{1}{2}\Delta)^2]F - \tfrac{1}{3}(E^2 - \tfrac{1}{4}U^2)^2 - \tfrac{3}{4}E^2(\tfrac{1}{2}\Delta)^2 = 0. \tag{54}$$

Depending on the values of $|t|$ and U the density of states may show a splitting. The quantity that determines this is the ratio of the bandwidth to the Coulomb repulsion $2Z|t|/U$, where Z is the coordination number. If we use Hubbard's criterion[13] that band splitting occurs when this ratio is ≤ 1.15, we find that below a dopant concentration of about 6×10^{18} phosphorous cm^{-3} one has two distinct Hubbard subbands separated by an energy gap. Since each phosphorus atom contributes exactly one donor electron the lower subband is completely filled while the upper one is entirely empty. Thus in this model the semiconductor-metal transition occurs at the donor concentration $n_{crit} \simeq 6\times10^{18}\,cm^{-3}$. The accepted experimental value of the donor density at which Si(P) undergoes a semiconductor-metal transition is 3×10^{18} phosphorus cm^{-3}. We attribute the discrepancy between the experimental and theoretical critical densities to the randomness in the distribution of the impurities, which we have ignored. This randomness produces band tailing and as a result the two Hubbard bands would begin to overlap at a lower impurity concentration than that predicted by our model.

The calculated density of states of the impurity band is of interest because experimentally one can extract information about this from the photoluminescent spectra, as explained in Sec. V. The intensity of the radiation arising from the recombination of electrons in the impurity band and free holes in the valence band is proportional to the convolution of the density of states of the impurity and valence bands. At low excitation levels only those valence-band states within approximately kT of the band maximum are unoccupied. Therefore at low temperatures the measured luminescent intensity due to recombination of impurity electrons and free holes is directly proportional to the density of states of the impurity band. In Fig. 4 we present a comparison between the experimentally observed impurity band and the density of states as calculated in the Hubbard model for the donor concentration 1.8×10^{18} and 3.9×10^{18} phosphorus cm^{-3}. As can be seen there is good agreement between the calculated and observed density of states, particularly for the concentration $1.8\times10^{18}\,cm^{-3}$. We attribute the discrepancy close to the band edges to band tailing which arises from the randomness of the impurity atoms.

We have also calculated the density of states of the impurity band assuming that the impurities fall into isolated pairs, following the treatment of Macek.[24] The donors are taken to be randomly distributed and the distance R between the impurities forming the hydrogen like molecule is assumed to follow the Chandrasekhar distribution.[25] The Heitler-London method[26] is used to set up the molecular wave functions in terms of the wave function (32) of the isolated donor and the expectation value of the molecular Hamiltonian evaluated. We take the envelope function to be spherically symmetric like (51), but with the effective Bohr radius a^* adjusted to give the asymptotic solution to the spherical-band effective-mass equation.[15] If intervalley terms are ignored, one obtains an expression for the energy which is identical to that given by the Heitler-London model for the hydrogen molecule. The density of states is then easily calculated. The result is shown in Fig. 4(a) for the donor concentration 1.8×10^{18} phosphorus cm^{-3}. The width of the impurity band obtained in this model is too narrow. If one of the donor electrons in the impurity molecule recombines with a free hole, then one is left with a dangling bond since in this model the molecule is assumed to be isolated. Thus the effect of correlation is overestimated. In reality, of course, the electron that is left behind would correlate with other elec-

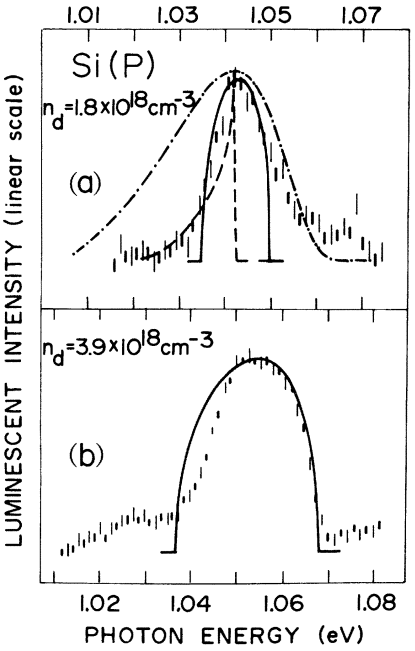

FIG. 4. Experimental and theoretical photoluminescent lines shapes for an electron in the impurity band and a free hole of phosphorus-doped silicon: (a) Sample containing 1.8×10^{18} cm^{-3}. Impurity-band line shapes at excitation levels of 5 W cm^{-2} (long flags) and 0.1 W cm^{-2} (short flags) are shown. The flags represent two standard deviations due to signal averaging and to the subtracting process referred to in Sec. V. The curves are the theoretical densities of states of the impurity band in the Hubbard (——), the Heitler-London (---), and the H_2^+ (-·-·-) models. They have been shifted in energy and scaled for comparison. (b) Sample containing 3.9×10^{18} cm^{-3}. Impurity-band line shapes at excitation levels of 20 W cm^{-2} (short flags) and 200 W cm^{-2} (long flags) are shown. The solid curve is the density of states of the impurity band in the Hubbard model. It has been shifted in energy and scaled for comparison with experiment.

trons.

It has been suggested by Lukes *et al.*[27] that the density of states of the impurity band may be calculated using the model of H_2^+ ion. We have also calculated the density of states in this model (again using the spherical-band approximation) and the result is shown in Fig. 4(a). The bandwidth obtained is far too broad and is a result of the fact that here correlations are entirely ignored.

IV. EXPERIMENTAL DETAILS

Single crystals of vacuum float zone phosphorus-doped silicon purchased from General Diode Corp. and Ventron Electronic Corp. were used. The impurity concentration was determined from room-temperature resistivity measurements. The samples were cut typically to $3\times5\times20$ mm^3 and etched for 30 sec in a mixture of HNO_3 and HF (5 : 1). The sample was immersed in liquid helium in an optical cryostat and the temperature could be varied by changing the helium vapor pressure. The optical excitation of the sample was varied over the range 0.1–200 W cm^{-2}.

To check that the sample was in thermal equilibrium with the helium bath, photoluminescent spectra were taken of intrinsic silicon under the same experimental conditions used in the measurement of the doped crystals. Analysis of the recombination emission attributed to free excitons[28] showed that the sample temperature is that of the helium bath for all optical excitation levels reported here.

For low excitation intensities a continuous He-Ne laser with 5-mW power output at 6328-Å wavelength was used; for higher excitations a continuous argon laser with a maximum power output of 2 W at 5145-Å wavelength was used. The irradiated area was a spot of 1-mm diameter. The recombination radiation was collected from the excited surface and analyzed with a 58-cm $f/3.5$ monochromator of Czerny-Turner design. A Bausch and Lomb Inc. grating blazed at 1.6 μm with 600 grooves/mm was used in the second order. An R.C.A. (67-07-B) germanium photodiode detector-preamplifier system operated at liquid-nitrogen temperature with detectivity $D^*(1.268\ \mu\text{m}, 91\ \text{Hz}, 1\ \text{Hz}) = 4.23\times10^{13}$ cm (Hz)$^{1/2}$/(rms W) and a noise equivalent power NEP(1.268 μm, 91 Hz, 1Hz) = 1.056×10^{-14} rms W/(Hz)$^{1/2}$ was used for signal detection. Further amplification was obtained with a low-noise preamplifier (PAR-113, Princeton Applied Research Corp.). The signal was then phase-sensitive detected (PAR-121 Lock-in, Princeton Applied Research Corp.) and integrated over times of typically 3 sec. The analog signal from the lock-in amplifier was electronically converted to a digital one and stored in the memory of a mini-computer (Nova 2, Data General Corp.). The mini-computer was interfaced[29] with the monochromator drive. This allowed programmable integration times as well as automatic signal averaging. The data were finally punched on paper tape at the end of the experiment for future analysis.

V. EXPERIMENTAL RESULTS AND ANALYSIS

In an indirect gap semiconductor such as silicon the radiative recombination must involve an additional process to conserve crystal momentum.[8,28] In phosphorus-doped silicon at 4.2 °K the strongest recombination emission is assisted by the simultaneous creation of a transverse-optical (TO) phonon.[8] For the purpose of clarity we will

only show in this paper the TO-phonon-assisted photoluminescent spectrum.

Figure 5(a) shows the spectrum of a sample containing 1.2×10^{17} phosphorus cm^{-3}. The excitation intensity is approximately 120 W cm^{-2}. The spectrum shows two overlapping peaks: A broad one at low energies attributed[8,30] to the EHD and a sharper one associated with an exciton bound to a neutral phosphorus impurity. Since the relative intensity of these peaks depends on the excitation level, the two overlapping peaks can be separated. The bound exciton (BE) peak strongly dominates the spectrum at very low excitation level (0.1 W cm^{-2}) and is used, properly scaled, to subtract the BE peak from the spectra obtained at excitation intensities in the range 10–200 W cm^{-2}. In this manner we obtain the EHD line shape, as shown in Fig. 5(b). The EHD line shape does not change in the range of excitation levels of interest. The solid curve in Fig. 5(b) shows a EHD theoretical line shape obtained by a convolution integral of the densities of state[31]

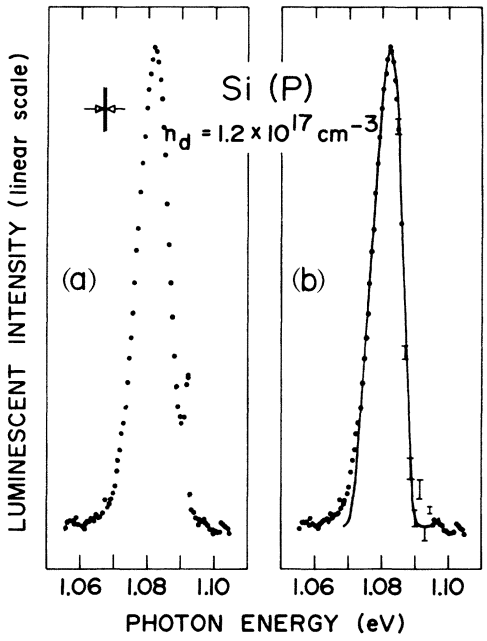

FIG. 5. (a) Photoluminescent spectrum of silicon containing 1.2×10^{17} phosphorus cm^{-3} at $T=4.2$ °K and 120 W cm^{-2} excitation level. The strong broad peak is attributed to the electron-hole drop (EHD), the weaker to the bound exciton (BE). (b) Solid circles show the experimental EHD line shape obtained by subtracting the BE line shape from the spectrum shown in (a). The errors in subtraction are shown. The solid curve is the theoretical fit to the EHD line shape.

$$I_{\mathrm{TO}}(h\nu)\propto\int_0^\infty\int_0^\infty N(E_e)N(E_h)f(E_e)f(E_h)\times\delta(h\nu-E_{\mathrm{pair}}+E_e^F+E_h^F-E_e-E_h+h\nu_{\mathrm{TO}})\,dE_e\,dE_h\,, \tag{55}$$

where E_e and E_h are, respectively, the electron and hole energies in the conduction and valence bands; $N(E_e)$ and $N(E_h)$ are the respective densities of state; $f(E_e)$ and $f(E_h)$ are the Fermi-Dirac distribution functions taken at the helium bath temperature; E_e^F and E_h^F are the Fermi energies for the electrons and holes; E_{pair}, as defined in Sec. II, is the energy required to add one more electron-hole pair to the EHD and is determined by the high-energy threshold of the luminescent peak. A theoretical fit has been performed by assuming the EHD to be charge neutral ($n_c=n_h+n_d$, see Sec. II) and by neglecting the nonparabolicity of the bands. The effective masses are assumed to be independent of doping and are given in Sec. II. We use 57.8 meV for the energy[28] of the TO phonon. As discussed in Sec. IV the sample temperature is that of the helium bath. The fit is performed by varying two parameters: E_{pair} which fixes the energy position and n_h which changes the line shape and width for a given impurity density (n_d). The parameters giving the best fit are shown in Figs. 2 and 3 as a function of impurity concentration.

The spectrum shown in Fig. 6 was obtained from a sample containing 5.7×10^{17} phosphorus cm^{-3}. The excitation intensity is approximately 160 W cm^{-2}. The line shape of the EHD peak centered at 1.0835 eV is independent of excitation intensity in the range 1–200 W cm^{-2} used in this experiment. The solid curve in Fig. 6 shows the theoretical fit. The BE peak (1.09 eV) is not observed. The peak appearing at low energy (1.061 eV) is attributed to the recombination of an electron in the impurity states with a free hole. Study of this peak at low excitation level is obscured by the appearance of a broad peak (~25 meV at half-intensity) at 1.042 eV which dominates the spectrum. We attribute this broad peak to donor-acceptor recombination because we observe a similar peak in samples doubly doped with boron and phosphorus. We have also studied samples with 3.1×10^{17} and 3.7×10^{17} phosphorus cm^{-3} intermediate to the impurity concentrations of samples discussed above. Our observations as a function of excitation level are in close agreement with those of Martin and Sauer[30] for a sample containing 1.8×10^{17} phosphorus cm^{-3}. A single recombination band is observed at high excitation intensity. With decreasing excitation level this band changes line shape and exhibits evidence of structure at low excita-

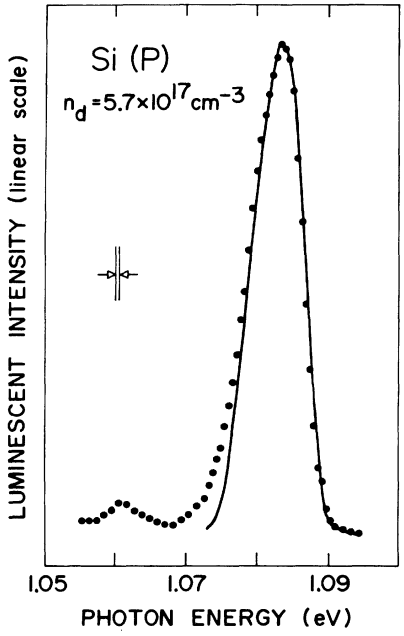

FIG. 6. The photoluminescent spectrum of silicon containing 5.7×10^{17} phosphorus cm^{-3} at $T = 4.2$ °K and 160 $W cm^{-2}$ excitation level is given by solid circles. The solid curve shows the theoretical fit to the EHD line shape.

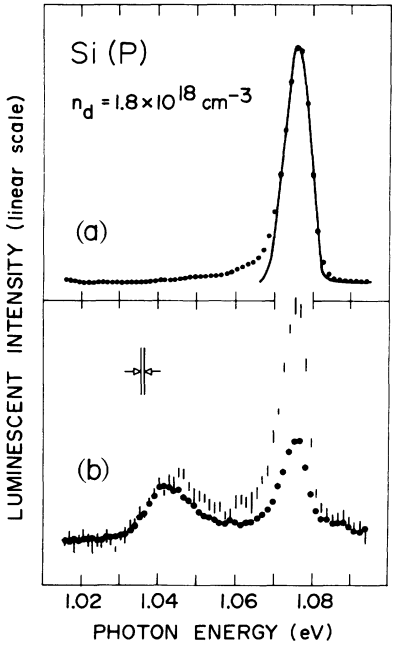

FIG. 7. Photoluminescent spectra of silicon containing 1.8×10^{18} phosphorus cm^{-3} at 4.2 °K. (a) Solid circles show the spectrum at high excitation level (200 $W cm^{-2}$). The peak is attributed to the EHD. The solid curve shows the theoretical fit to the EHD line shape. (b) The flags (two standard deviations from 6 scans) show the spectrum at intermediate excitation level (20 $W cm^{-2}$) and the solid dots (50 scans) the spectrum at low level (0.1 $W cm^{-2}$). The peak at high energies is attributed to the EHD, the other to the impurity band. The spectra have been scaled for comparison.

tion intensity. Martin and Sauer[30] argue that these changes in line shape were indicative of a profound change in the electronic states. We think that an alternative explanation is that the BE peak is very broad and overlaps the EHD peak to form a single broad band. The changes in this band with excitation level can be attributed to the change in the relative intensities of the EHD and BE emissions with excitation level.

In our previously published experimental work[9] we have shown spectra for samples containing 1.8×10^{18}, 3.0×10^{18}, and $3.9 \times 10^{18} cm^{-3}$. A detailed analysis of those data will be presented here. Each spectrum shows two peaks. As previously reported the peak at high photon energy is attributed to recombination within the EHD. The other peak is attributed to recombination of an electron in the "impurity band"[12] with a free hole. The impurity band (IB) peak shifts to higher energy as the impurity concentration increases. The relative intensities of the two peaks depends on the excitation level. The EHD peak dominates the spectrum at high excitation level; the IB peak dominates at low level.

Figure 7 shows the spectra of a sample containing 1.8×10^{18} phosphorus cm^{-3}. Figure 7(a) shows the spectrum at high excitation level (200 $W cm^{-2}$). The solid curve shows the theoretical fit to the EHD line shape. Figure 7(b) shows the spectra at intermediate (20 $W cm^{-2}$) and low (0.1 $W cm^{-2}$) excitation levels. The spectra in this figure have been scaled so that the low-energy tails of the IB peaks are superimposed. The line shape of the EHD peak obtained by subtracting these two spectra is the same as the one obtained at high excitation intensities shown in Fig. 7(a). The line shape of the IB peak is obtained by subtracting the EHD line shape [Fig. 7(a)] from the low excitation level (0.1 $W cm^{-2}$) spectrum. As shown in Fig. 4(a) the same IB line shape is obtained by subtracting the EHD line shape from an intermediate excitation (5 $W cm^{-2}$) spectrum. We assume that the recombination emission of electrons in the impurity band and free holes in the valence band is proportional to the convolution of the densities of state of the two bands. Since only those states of the valence band within approximately kT of the band maximum are unoccupied at 4.2 °K and this energy is negligible compared to the width of the observed IB peak, the experimental IB line shape gives directly the density of states in the impurity band. In Sec. III the impurity band has been discussed in terms of the

Hubbard model. The calculated density of states of the completely filled lower Hubbard band is shown by the solid curve in Fig. 4(a). Also shown in Fig. 4(a) are the calculated densities of state in the Heitler-London and H_2^+ models. The theoretical bands have been shifted in energy and scaled.

Figure 8(a) shows two spectra of a sample containing 3.9×10^{18} phosphorus cm^{-3}. The high excitation-level spectrum (200 W cm^{-2}) shows both the EHD and the IB peaks. In the low-level spectrum (0.2 W cm^{-2}) the IB peak strongly dominates the spectrum. The line shape of the EHD peak obtained by subtracting these two spectra is shown in Fig. 8(b). We have also obtained the EHD line shape as a function of excitation levels in the range 10–200 W cm^{-2}. The EHD line shape is not observed to change with excitation level. The solid curve in Fig. 8(b) shows the theoretical fit to the EHD peak. The two superimposed IB peaks shown in Fig. 4(b) were obtained by subtracting the EHD line shape [Fig. 8(b)] from intermediate (20 W cm^{-2}) and high-excitation-level (200 W cm^{-2}) spectra. The line shape is not observed to change in this range of excitation intensities and is very nearly that observed in the low-level excitation

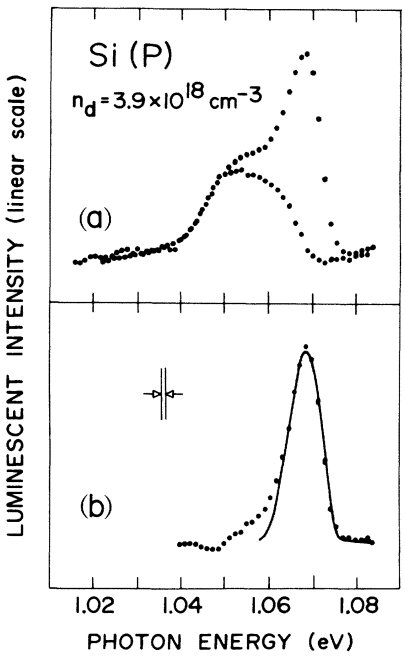

FIG. 8. (a) Photoluminescent spectra of silicon containing 3.9×10^{18} phosphorus cm^{-3} at $T=4.2$ °K are shown at two excitation levels. At high excitation level (200 W cm^{-2}, 1 scan) both the impurity band (IB) and the EHD peaks are observed and at low level (0.2 W cm^{-2}, 60 scans) the IB peak strongly dominates. (b) The solid circles give the EHD line shape obtained by subtracting the two spectra in (a). The solid curve shows the theoretical fit to the EHD line shape.

spectrum. As discussed in Sec. III the solid curve in Fig. 4(b) is the density of states in the Hubbard model.

The spectrum of the sample containing 1.8×10^{18} cm^{-3} shown in Fig. 4(a) has been shifted by 8 meV with respect to the spectrum of the sample containing 3.9×10^{18} cm^{-3} shown in Fig. 4(b) for comparison. Little change is observed in the low-energy tail of the IB line shape. A larger half-width is observed for the higher concentration. The line shape of the IB peak for the low impurity concentration shows a high-energy tail. This tail is not observed at high impurity concentration; in fact an edge is observed. The data of samples containing 2.45×10^{18} cm^{-3} and the previously reported[9] 3.0×10^{18} cm^{-3} are intermediate to the ones under discussion and will not be shown here. The EHD and the IB peaks have been separated and the results of the analysis are intermediate to those found above.

The half-width increase with concentration is theoretically expected[13] in the Hubbard model. As discussed in Sec. III this model predicts the semiconductor-metal transition when the completely filled Hubbard band starts to overlap the empty upper Hubbard band. For donor concentrations above n_{crit} (3×10^{18} cm^{-3}) a single half-filled band is expected and the high-energy edge of the impurity band peak of the sample containing 3.9×10^{18} cm^{-3} is evidence of this partial filling.

The data and analysis of a sample containing 5.0×10^{18} cm^{-3} will not be shown here since they may be inferred from those of the previously discussed sample containing 3.9×10^{18} cm^{-3} and those of the 1.1×10^{19} cm^{-3} to be discussed below.

For samples containing impurity concentrations above 5×10^{18} cm^{-3} n_h is significantly less than n_c and consequently the theoretical half-width of the EHD line shape is not sensitive to changes in n_h. The fit to the high-energy edge of the EHD line shape is essential. Mahler and Birman[11] have chosen to compare their theoretical calculations with the experimental half-widths obtained by Halliwell and Parsons.[8] In the region where their approach is valid ($n_d < 5\times10^{18}$ cm^{-3}) the present experimental data show that the half-widths of the EHD line shape are less than those previously published[8] due to the fact that we are now able to resolve the EHD and IB peaks.

Figure 9 shows the spectra of a sample containing 1.1×10^{19} cm^{-3}. The excitation intensities are (a) high (150 W cm^{-2}), (b) intermediate (20 W cm^{-2}), and (c) low (2 W cm^{-2}). The EHD peak very strongly dominates the high-excitation-level spectrum. The IB peak very strongly dominates the low-level one. The photoluminescent intensity for samples with impurity concentrations

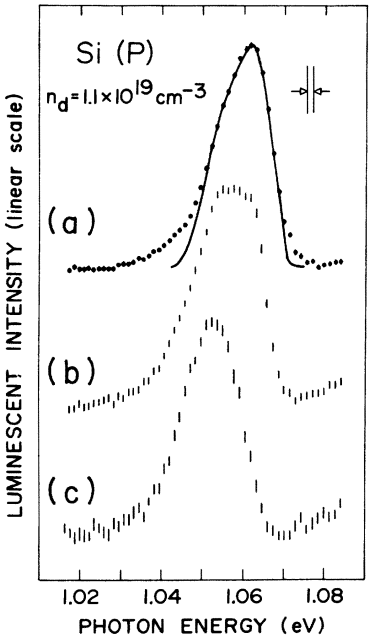

FIG. 9. Photoluminescent spectra of silicon containing 1.1×10^{19} phosphorus cm^{-3} at $T = 4.2$ °K are shown at three excitation levels. (a) At high excitation level (150 W cm^{-2}, 5 scans) the EHD peak dominates the spectrum. The solid curve shows the theoretical fit to the EHD line shape. (b) At intermediate level (20 W cm^{-2}, 15 scans) both the IB and EHD peaks are observed. (c) At low level (2 W cm^{-2}, 35 scans) the IB peak dominates the spectrum.

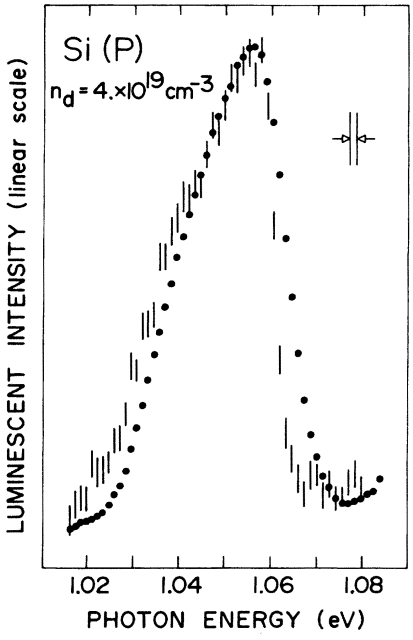

FIG. 10. Photoluminescent spectra of silicon containing 4×10^{19} phosphorus cm^{-3} at $T = 4.2$ °K are shown at two excitation levels. The solid points show a high excitation level (150 W cm^{-2}, 10 scans) spectrum. The flags correspond to low level (5 W cm^{-2}, 110 scans).

above n_{crit} decreases strongly with increasing concentration and in addition the relative intensity of the EHD and IB peaks becomes more strongly dependent on excitation level. As shown in Fig. 9(c), only the IB peak is observed at low excitation level. Except for a slightly steeper high-energy edge the IB line shape in Fig. 9(c) is the same as that obtained for samples containing 3.9×10^{18} cm^{-3} [shown in Fig. 4(b)] and 5.0×10^{18} cm^{-3} (not shown). The solid curve in Fig. 9(a) shows the theoretical fit to the EHD peak. The EHD line shape is independent of excitation level in the range 80–200 W cm^{-2}. The spectrum at intermediate excitation intensity [Fig. 9(b)] can be reproduced by adding the high-excitation-level spectrum [Fig. 9(a)] to the low-level one [Fig. 9(c)], properly scaled.

For phosphorus-doped silicon a second characteristic concentration,[19] $n_{cb} \simeq 2 \times 10^{19}$ cm^{-3}, is evidenced in the measurement of the Knight shift of the NMR absorption peak for ^{29}SI as a function of impurity concentration. Alexander and Holcomb[19] argue that the Fermi level is above the conduction band edge for impurity concentrations greater than n_{cb}.

Figure 10 shows two spectra of a sample containing 4.0×10^{19} cm^{-3}. High (150 W cm^{-2}) and low (5 W cm^{-2}) excitation intensities have been used. The line shape of the observed peak depends on the excitation intensity within the range 5–200 W cm^{-2}. The line shape of the peak shows a decrease in the slope of the low- and high-energy side with increasing excitation level. These changes in line shape with excitation level could be interpreted in terms of unresolved broad EHD and IB peaks; however, one cannot make firm conclusions because of the absence of structure in the photoluminescent spectrum for 4.0×10^{19} cm^{-3}. We were unable to fit a theoretical EHD line shape to any of the spectra obtained at this concentration.

VI. SUMMARY AND CONCLUSION

We have studied the photoluminescent spectrum of Si(P) over a wide range of impurity concentration. The spectrum is a sum of two components: one arising from electron-hole recombination events within the droplet, and the other arising from the recombination of electrons in the impurity band with holes in the valence band. The former type of events dominates the spectrum at high excitation intensities and the latter at low excitation levels. By studying the photoluminescence spectrum at various excitation intensities, we have been able to disentangle the two contributions and extract the

density of states of the impurity band.

We have extended the theory of electron-hole droplets in heavily doped Si. The calculated values of the average energy per charge-carrier pair within the droplet are in good agreement with the experimental values obtained from the high-energy edge of the EHD recombination peak. We have calculated the impurity-band density of states below the critical density for the semiconductor-metal transition in the Hubbard model. Again, good agreement was found with experiment.

The effect of randomness of the distribution of donor atoms on the density of states of the impurity band has been ignored in this paper. Also a reliable theoretical determination of the minority carrier density n_h in the intermediate density region would require a more accurate determination of the impurity and correlation energies than we have been able to present here. We plan to come back to these questions elsewhere.

ACKNOWLEDGMENTS

We are grateful for many helpful suggestions from R. Barrie and M. L. W. Thewalt. We wish to thank H. Gush for the loan of a Ge detector, and T. M. Rice for discussions on several aspects of the problem. We also wish to thank K. F. Berggren for a helpful correspondence. This research was supported by the National Research Council of Canada. One of the authors (P. J.) is also thankful to the National Science Foundation through the Northwestern University Materials Research Center for financial support.

APPENDIX: DEPENDENCE OF THE MINORITY-CARRIER DENSITY ON DONOR IMPURITY CONCENTRATION IN THE HARTREE-FOCK APPROXIMATION

In order to understand better the physical origin of the dip in the equilibrium density of holes inside the electron-hole liquid at intermediate dopant concentration, we consider the energetics of the situation in the Hartree-Fock approximation. The kinetic and exchange contributions to the energy per unit volume are, respectively,

$$E_{\rm kin} = c_1(n_d + n_h)^{5/3} + c_2 n_h^{5/3},$$
$$E_{\rm exc} = -d_1(n_d + n_h)^{4/3} - d_2 n_h^{4/3}. \tag{A1}$$

Here

$$c_1 = \frac{\pi^{4/3}3^{5/3}\hbar^2}{10(m_{lc}m_{tc})^{1/3}\nu^{2/3}} = 0.331\times10^{-26}\ \text{erg cm}^2,$$

$$c_2 = \frac{\pi^{4/3}3^{5/3}\hbar^2}{10(m_{\rm lh}^{3/2} + m_{\rm hh}^{3/2})^{2/3}} = 0.649\times10^{-26}\ \text{erg cm}^2,$$

$$d_1 = \frac{3^{4/3}e^2\Phi}{4\pi^{1/3}\epsilon(0)\nu^{1/3}} = 0.773\times10^{-20}\ \text{erg cm}, \tag{A2}$$

$$d_2 = \frac{3^{4/3}e^2\psi}{4\pi^{1/3}\epsilon(0)} = 1.106\times10^{-20}\ \text{erg cm}. \tag{A3}$$

Here ν is the number of conduction-band valleys ($\nu = 6$ for Si) and the functions Φ and ψ are given explicitly in Ref. 3. Substitution of (A1) into expression (11) for $\overline{E}$ and differentiation with respect to n_h gives

$$n_d^{1/3}\left\{c_1\left[\frac{5}{3}\frac{n_h}{n_d}\left(1+\frac{n_h}{n_d}\right)^{2/3} - \left(1+\frac{n_h}{n_d}\right)^{5/3} + 1\right] + \tfrac{2}{3}c^2\left(\frac{n_h}{n_d}\right)^{5/3}\right\}$$
$$= d_1\left[\frac{4}{3}\frac{n_h}{n_d}\left(1+\frac{n_h}{n_d}\right)^{1/3} - \left(1+\frac{n_h}{n_d}\right)^{4/3} + 1\right]$$
$$+ \tfrac{1}{3}d_2\left(\frac{n_h}{n_d}\right)^{4/3}. \tag{A4}$$

We note from (A4) that its solutions will behave qualitatively differently depending on whether $n_d^{1/3}c_1$ or $n_d^{1/3}c_2$ is much smaller or much greater than d_1 and d_2. The critical region is around $n_d \sim 10^{18}\ \text{cm}^{-3}$. For low impurity concentrations ($n_d \ll 10^{18}\ \text{cm}^{-3}$) $n_h \gg n_d$, while for high concentrations $n_h \ll n_d$. By Taylor expanding both sides of (A4) we get in the two regimes

$$n_h \approx \frac{1}{8}\left(\frac{d_1+d_2}{c_1+c_2}\right)^3 + n_d\left(\frac{-8d_1}{d_1+d_2} + \frac{5c_1}{2(c_1+c_2)}\right)$$
$$(\text{for } n_d \gg 10^{18}\ \text{cm}^{-3})$$
$$= 0.88\times10^{18}\ \text{cm}^{-3} - 2.4n_d \tag{A5}$$

and

$$n_h \approx \left(\frac{d_2}{2c_2}\right)^3 - \frac{5c_1}{2c_2}\left(\frac{d_2}{2c_2}\right)^{4/3} n_d^{-1/3}, \quad \text{for } n_d \gg 10^{18}\ \text{cm}^{-3}$$
$$= 6.2\times10^{17}\ \text{cm}^{-3} - 6.7\times10^{23} n_d^{-1/3}\ \text{cm}^{-4}. \tag{A6}$$

On the whole the exchange contribution favors condensation while the kinetic-energy contribution has the opposite effect. Both effects are weakened when the impurities are present. At low impurity concentration it turns out that it is the exchange energy that is most affected. The net effect is a lowering of the quasiequilibrium minority-carrier density. At very high impurity concentration the energetics of droplet formation is dominated by the valence-hole contributions and the quasiequilibrium hole density approaches a constant value. If now the impurity concentration is reduced the kinetic-energy "cost" and exchange-energy "gain" associated with the conduction electrons both increase in

importance. However, this time it turns out that the change in the kinetic energy is most important.

It should be emphasized that the minimum in $\bar{E}$ at the quasiequilibrium is quite shallow in the intermediate impurity-density regime. The density is therefore quite sensitive to correction terms that go beyond the Hartree-Fock approximation.

[1]See, e.g., C. D. Jeffreys, Science 189, 955 (1975) for a recent general review.

[2]Ya. E. Pokrovski, Phys. Status Solidi A 11, 385 (1972).

[3]C. Benoît à la Guillaume, M. Voos, and F. Salvan, Phys. Rev. B 5, 3079 (1972).

[4]M. Combescot and P. Nozières, J. Phys. C 5, 2369 (1972).

[5]M. Inoue and E. Hanamura, J. Phys. Soc. Jpn. 34, 652 (1973).

[6]W. F. Brinkman and T. M. Rice, Phys. Rev. B 7, 1508 (1973).

[7]P. Bhattacharyya, V. Massida, K. S. Singwi, and P. Vashishta, Phys. Rev. B 10, 5127 (1974).

[8]R. E. Halliwell and R. R. Parsons, Solid State Commun. 13, 1245 (1974); Can. J. Phys. 52, 1336 (1974).

[9]J. A. Rostworowski, M. L. W. Thewalt, and R. R. Parsons, Solid State Commun. 18, 93 (1976).

[10]B. Bergersen, P. Jena, and A. J. Berlinsky, J. Phys. C 8, 1377 (1975).

[11]G. Mahler and J. L. Birman, Solid State Commun. 17, 1381 (1975); Phys. Rev. B 12, 3221 (1975).

[12]W. Baltensberger, Philos. Mag. 44, 1355 (1953).

[13]J. Hubbard, Proc. R. Soc. A 276, 238 (1963); *ibid.* A 281, 401 (1964).

[14]K.-F. Berggren, Philos. Mag. 27, 1027 (1973).

[15]W. Kohn, in *Solid State Physics*, edited by F. Seitz and D. Turnbull (Academic, New York, 1957), Vol. 5, p. 257.

[16]S. T. Pantelides and C. T. Sah, Phys. Rev. B 10, 621 (1974); A. Baldereschi, Phys. Rev. B 1, 4673 (1970).

[17]M. Combescot and P. Nozières, Solid State Commun. 10, 301 (1972).

[18]H. Nara and A. Morita, J. Phys. Soc. Jpn. 21, 1852 (1966).

[19]M. N. Alexander and D. F. Holcomb, Rev. Mod. Phys. 40, 815 (1968).

[20]R. L. Aggarwal and A. K. Ramdas, Phys. Rev. 140, A1246 (1965).

[21]The "previous results" are those of Ref. 10 except that we have corrected a small numerical error in E_{imp}.

[22]Mahler *et al.* (Ref. 11) do not include E_{imp} in their energy minimization. Further, they discriminate between loosely and tightly bound donor electrons: The latter are ignored in the energy minimization procedure, but are phenomenologically included in their calculation in a pressure term. We disagree with the way this term is included in Eq. (31) of Ref. 11. The authors assume a condition for mechanical equilibrium which in our notation would read $E(n_d, 0) = n_d \partial E(n_d, 0)/\partial n_d$, somewhat in analogy with our Eq. (11). However, the donor ions in silicon are not in equilibrium in this sense. If the donor ions were free to diffuse only one particular donor concentration would have been possible, but in the actual samples the donor concentration is kept frozen and we do not have mechanical equilibrium in the sense assumed in Ref. 11.

[23]A. Miller and E. Abrahams, Phys. Rev. 120, 745 (1960).

[24]V. Macek, Ph.D. thesis (University of British Columbia, 1971) (unpublished).

[25]S. Chandrasekhar, Rev. Mod. Phys. 15, 1 (1943).

[26]See, for example, J. C. Slater, *The Quantum Theory of Matter*, 2nd ed. (McGraw-Hill, New York, 1968), p. 414.

[27]T. Lukes, B. Nix, and B. Suprapto, Philos. Mag. 26, 1239 (1972).

[28]P. J. Dean, J. R. Haynes, and W. F. Flood, Phys. Rev. 161, 711 (1967).

[29]M. L. W. Thewalt, M.Sc. thesis (University of British Columbia, 1975) (unpublished).

[30]R. W. Martin and R. Sauer, Phys. Status Solidi B 62, 443 (1974).

[31]C. Benoît à la Guillaume and M. Voos, Phys. Rev. B 7, 1723 (1973).